Proceedings of the ASME 2011 9th International Conference on Nanochannels, Microchannels, and Minichannels
ICNMM2011
June 19-22, 2011, Edmonton, Alberta, CANADA

ICNMM2011-58159

A ROBUST SUPERHYDROPHOBIC SURFACE FOR DIGITAL MICROFLUIDICS

David Barona
Dept. of Mechanical Engineering
University of Alberta
Edmonton, Alberta, Canada

A. Amirfazli*
Dept. of Mechanical Engineering
University of Alberta
Edmonton, Alberta, Canada

ABSTRACT

Digital microfluidics depends on efficient movement of individual drops for a variety of tasks, e.g. reagent delivery, mixing, sampling, etc. Superhydrophobic (SH) coatings generally show high repellency and low adhesion for a variety of liquids. Therefore, SH coatings can provide for an efficient drop delivery and hence low energy requirements for a fluidic chip. However, wide application of such coatings is hampered by fragile nature of such coatings to date. A new SH coating is developed that addresses the fragility challenge of such coatings. It is based on application of nanoparticles to fluoropolymers. The mechanical stability, wear resistance and durability under prolonged liquid exposure of this new coating is discussed. It is shown that the new SH coating can maintain high contact angles, low contact angle hysteresis needed for drop mobility under adverse conditions/application of digital microfluidic devices. The developed SH coating can also be sprayed onto various surfaces, including glass used in traditional lab-on-chip (LOC) devices, or even paper for enabling novel Lap-on-paper (LOP) devices.

INTRODUCTION

Research in the area of digital microfluidics has largely focused on the movement of drops across a surface whose hydrophobicity is changed mainly by the use of electric fields to temporarily create a polarized hydrophilic surface. This is commonly referred to as electrowetting (*1*,*2*). Recently research has been exploring alternative lab-on-chip (LOC) devices such as lab-on-paper (LOP) devices. LOP devices are useful due to paper's versatile, inexpensive and biodegradable character (*3*,*4*). For any of these devices, drop repellency, adhesion and mobility are best characterized and understood through contact angle and contact angle hysteresis (*5*,*6*). Other important aspects such as the stability of wetting modes (Cassie or Wenzel) and the transitions between them are also of concern and have been well studied in the past fifteen years (*7*,*8*,*9*,*10*).

Although previously studied surfaces exhibited favorable mechanical properties and resistance to abrasion, their hydrophobic performance significantly decreased when continuously exposed to water for ~5 minutes (*3*). The focus of this study was to study a more robust nanocomposite SH sprayable coating and understand its resistance to abrasion and water immersion.

MATERIALS AND METHODS

The SH coating used in this study is inspired by methodology of using nano- and mirco-particles in conjunction with a fluoropolymer and adhesive to create a rough hydrophobic surface, e.g. see (*11*). In this study, the formulation from our previous study (3) was changed by using a different water resistant adhesive, which was mixed with fluorinated polyurethane as the fluorinated sealant and the addition of Teflon AF. This newest formulation (called B21) has been sprayed in four different variations as shown in Table 1 onto three different substrates: 0.4mm thick 6061T6 aluminum, 1.0mm thick microscope glass slides and a 1.0mm thick polymeric composite material made from pre-impregnated reinforcing fibers with a partially cured polymer matrix resin (*12*). Thicknesses of coating layers on microscope glass slides were measured with a micrometer at three different locations. The combination of four different treatments on three different substrates (12 samples total) helps us examine how the coating's mechanical properties and adhesion differ from case to case. Note that superhydrophobicity is a function of surface chemistry and its roughness (*13*), so altering any of these two

**Department of Mechanical Engineering, University of Alberta, Edmonton, Alberta T6G-2G8, Canada. E-mail: a.amirfazli@ualberta.ca; Tel: +1 (780) 492-6711*

characteristics can influence the wetting behavior. In this particular case, changes to the surface's chemistry are not expected to play a significant role due to the main components used being water repellent or water resistant. Therefore, most of the changes to the coating's performance are expected to originate from changes to the coating's roughness (impacted by abrasive wear), the coating's adhesion to the substrate and the strength of the cured coating itself (impacted by prolonged exposure to water).

The study was carried out in three parts. The first part involved spraying the four different treatments on the three different substrates and characterizing their wetting behavior through contact angle (CA) measurements. The different treatments of the coating were sprayed using an internal mixing airbrush (Aztek A3208 with a 0.50mm high flow nozzle at 414 kPa) achieving the thicknesses shown in Table 1. The thin coat treatments, B21 (one thin coat of B21) and 2XB21 (two thin coats of B21) were achieved using the nozzle in its original configuration. An internal pin within the nozzle was removed to allow for a larger mass flow rate, resulting in the thicker coat treatments B21T (one thick coat of B21) and 2XB21T (two thick coats of B21). Each treated substrate cured in an oven at 90˚C for 2 hours and allowed to remain and stabilize for a period of at least 6 hours prior to any further handling or testing. The samples were then tested for wetting by measuring advancing and receding contact angles. Images of drops ranging from 5-40μL were acquired with a custom built setup for an average wetting test duration of ~20 seconds. The relatively large size of the drops (5-40μL) has been shown to have negligible differences in contact angle measurements when compared to smaller drop volumes of 3-10μm (*3*). The in-house built set-up used consists of a stationary plate where an individual sample is placed. In this study, drops were placed from above using a 250μL syringe that is attached to a motor controlled by a computer. A CCD camera and a light source are mounted opposite to each other on an arm with the sample at its center. This set-up allows us to obtain advancing and receding contact angles by adding or removing liquid, respectively, to or from a drop for a variety of substrates. Contact angles were measured using the DropSnake (*14*) plug-in for ImageJ for Mac OS X. This plug-in uses cubic-spline interpolation to determine the precise location of the profile of the drop as well as the contact points with the substrate used together to compute the contact angle of the drop. Two contact angle measurements (left and right contact points) were taken from each of the 15-20 images obtained from each treated substrate for a total of 30-40 independent measurements.

Table 1 Details for the different treatments of B21 applied to the aluminum, glass and composite substrates. Three different thickness measurements were taken at three different locations for each treatment.

Treatment	*Thickness (μm)*	*Description*
B21	24.5 ± 3.6 μm	One coat of B21
2XB21	56.7 ± 2.9 μm	Two coats of B21
B21T	52.9 ± 2.6 μm	One thick coat of B21
2XB21T	95.3 ± 4.4 μm	Two thick coats of B21

The second part of this study involved subjecting two of the treated aluminum samples (2XB21 and B21T) to several wear intervals to examine the surface's mechanical robustness. The wear testing equipment consists of a gyratory shaker table modified to accommodate a pan filled with abrading material with a relative motion of ~0.5cm to the target sample. At the bottom of the pan, there is a recessed section into which a sample to be worn fits such that it sits flush with the bottom of the pan. The pan was designed this way so that the flow of abrading particles is smooth and uninterrupted by any protrusions or edge effects introduced by the sample itself. After securing the sample to the testing device, the pan is filled with abrading material for a depth of 2.54cm. For this particular case, ~0.5-1.0mm diameter glass beads commonly used for sand blasting were chosen as the abrading material. Such glass beads are also ideal since they leave little to no contamination on the worn surface. Any contamination left can be easily blown off with dry nitrogen. Once the sample and particles are in place, the machine is turned on at a speed or 250rpm for the desired amount of time. For this particular study, the samples tested (2XB21 and B21T treated aluminum) were worn for a cumulative 5, 30, 60, 120 and 240 minutes. The performance of the coating on each sample is characterized by performing the wetting tests previously described after each wear interval.

The third part of this study involved immersing the 12 treated surfaces in deionized water for 5.5 hours to study any changes to coating's performance. Changes to the wetting behavior are expected to come from changes to the morphology of the surface or to the adhesion of the coating to the substrate. After the immersion period, the samples were blown with dry nitrogen to remove any excess water and allowed to completely dry for a period of at least 6 hours in an oven at 50˚C. After the immersion and drying cycle is completed, the repellency of the coating on each sample is characterized by performing the wetting tests previously described.

RESULTS AND DISCUSSION

The first part of this study dealt with the spraying and wetting characterization of the newly formulated B21 nanocomposite SH coating. The different coat thicknesses are shown in Table 1 whereas the contact angles for each of the 12 different treatment/substrate combinations (unworn and unimmersed) are shown in Table 2. It can also be seen from Table 2 that for each substrate set, the samples coated with the 1-coat treatments (B21 and B21T) show the largest hysteresis. This larger hysteresis, when compared two the 2-coat treatments (2XB21 and 2XB21T), exists likely due to the presence of flat areas (defects) on the surface. It can be seen in the SEM images (Fig. 1) that some of the underlying substrate is not fully covered by the particles in the 1-coat treatments (Fig. 1a and c).

Table 2 Contact angle measurements for the 12 different treatment/substrate combinations. Different contact angles for the same treatment on different substrates suggest that the roughness of the bare substrate along with its chemistry cannot be ignored, especially for the 1-coat treatments (B21 and B21T).

	Treatment	*Advancing CA (deg.)*	*Receding CA (deg.)*	*CA Hysteresis (deg.)*
Aluminum	*B21*	160.3˚ ± 5.5˚	128.8˚ ± 18.8˚	31.5˚ ± 19.5˚
	2XB21	155.9˚ ± 6.5˚	140.3˚ ± 10.2˚	15.7˚ ± 12.1˚
	B21T	156.9˚ ± 6.4˚	131.3˚ ± 9.1˚	25.6˚ ± 11.1˚
	2XB21T	158.8˚ ± 4.7˚	141.7˚ ± 13.6˚	17.1˚ ± 14.4˚
Composite	*B21*	162.6˚ ± 3.8˚	145.0˚ ± 10.2˚	17.6˚ ± 10.9˚
	2XB21	159.5˚ ± 2.6˚	147.5˚ ± 5.1˚	12.0˚ ± 5.7˚
	B21T	160.3˚ ± 2.4˚	145.4˚ ± 4.7˚	14.9˚ ± 5.3˚
	2XB21T	157.9˚ ± 3.8˚	146.0˚ ± 9.4˚	12.0˚ ± 10.1˚
Glass	*B21*	158.0˚ ± 2.8˚	146.5˚ ± 9.6˚	11.6˚ ± 10.0˚
	2XB21	160.0˚ ± 4.1˚	152.3˚ ± 8.8˚	7.7˚ ± 9.7˚
	B21T	152.9˚ ± 4.4˚	121.5˚ ± 10.1˚	31.4˚ ± 11.0˚
	2XB21T	155.4˚ ± 6.1˚	140.2˚ ± 7.1˚	15.2˚ ± 9.4˚

The second portion of this study focused on conducting wear tests on two of the treated aluminum samples: 2XB21 and B21T. Treatment 2XB21 was chosen because it covers the substrate very well (see Fig. 1b) leaving no apparent portions of the flat underlying substrate. This allows for the wear tests conducted to properly examine the mechanical robustness of the coating. On the other hand, B21T was chosen as the second treatment to wear because it leaves some of the substrate exposed while containing enough material for a similarly long amount of wear (thicknesses are within ~4µm of 2XB21 as shown in Table 1). Wearing two different treatments of similar thicknesses would provide clearer insight into which features of each treatment make one more robust than the other.

The two treated samples were subjected to cumulative amounts of wear of 5, 30, 60, 120 and 240 minutes with their contact angles plotted in Fig. 2. It can be seen from the data collected that for both treatments, after 240 minutes of wear, hysteresis increases to ~40˚. However, repellency, related to the advancing contact angles, remains above 140˚ for the duration of the test. On the other hand, mobility, related to contact angle hysteresis is different for the two tested samples. As shown in Fig. 2b, contact angle hysteresis increases above 20˚ within the first ~5 minutes of wear, whereas Fig. 2a shows the same increase within the first ~60 minutes of wear. This quick increase in contact angle hysteresis can be attributed to the fact that more of the underlying aluminum is being exposed as wear goes on. Nonetheless, advancing contact angles above 140˚ and receding contact angles above 90˚ describe surfaces that could allow good movement of drops for mixing, transportation and sampling purposes in the context of LOC devices as has been previously shown (*3*).

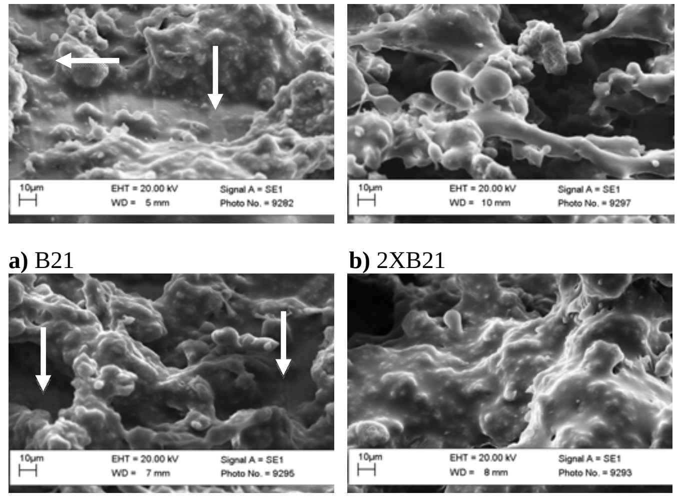

a) B21 **b)** 2XB21 **c)** B21T **d)** 2XB21T

Fig. 1 SEM images of the four different treatments on an aluminum substrate at 1000X magnification prior to being worn or immersed. White arrows point to uncoated/exposed areas of the underlying substrate in the 1-coat treatments (B21 and B21T). When exposed areas of the substrate come in contact with the wetting drops, contact angles are reduced since the substrates are not hydrophobic.

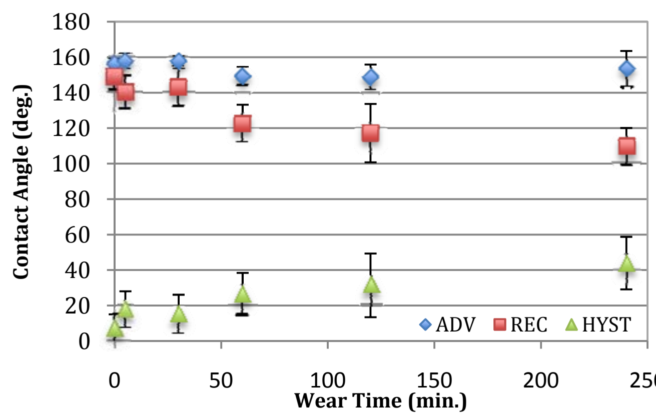

a) Aluminum treated with 2XB21

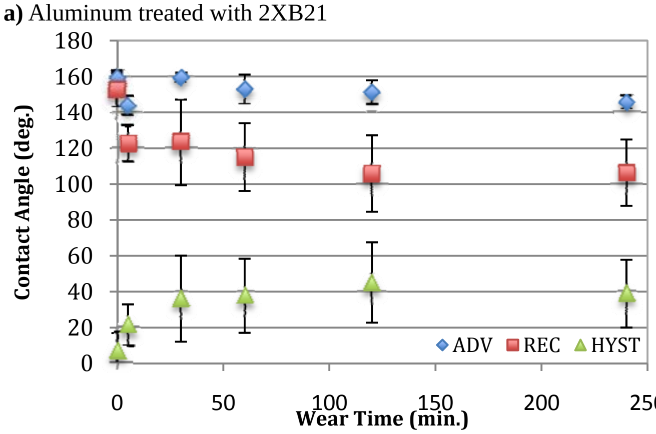

b) Aluminum treated with B21T

Fig. 2 Plots of the changes in wetting behavior for a) 2XB21 and b) B21T after subject to wear at 250rpm for a cumulative time of 240 minutes. Plots show that B21T experiences an increase in CA hysteresis earlier than 2XB21, largely corresponding to more of the aluminum being exposed.

The third portion of this study focused on continuously immersing the treated samples to deionized water for hours at a time. A previous study had shown that the SH coating developed at the time lost its hydrophobic properties after being immersed in water for ~5 minutes (*3*)**.** However, the B21 variant of the SH coating only starts to show a notable decrease in performance after 5.5 hours of continuous water immersion: considerably longer durability when compared to what had been previously observed. Contact angle measurements for all 12 samples are shown in Table 3.

It can be seen from the data in Table 3 that after 5.5 hours of continuous immersion in water, advancing contact angles remain above 140˚, which corresponds to the early portion of the SH regime. This means that after this prolonged period of exposure, the samples maintain high repellency. On the other hand, receding contact angles are significantly lower, but remain above 100˚ and in the hydrophobic regime.

Table 3 Contact angle measurements for the 12 different treatment/substrate combinations after 5.5 hours of immersion. Contact Angle Hysteresis Δ shows the positive change in hysteresis observed after the immersion period.

	Treatment	*Advancing CA (deg.)*	*Receding CA (deg.)*	*CA Hysteresis (deg.)*	*CA Hyst Δ (deg.)*
Aluminum	***B21***	145.2˚ ± 6.4˚	112.8˚ ± 15.5˚	32.4˚ ± 16.7˚	0.9˚
	2XB21	151.4˚ ± 13.3˚	113.6˚ ± 11.9˚	37.8˚ ± 17.9˚	22.1˚
	B21T	146.6˚ ± 9.4˚	109.2˚ ± 19.9˚	37.5˚ ± 22.0˚	11.9˚
	2XB21T	153.6˚ ± 7.3˚	111.2˚ ± 13.9˚	42.3˚ ± 15.7˚	25.2˚
Composite	***B21***	158.2˚ ± 5.4˚	125.9˚ ± 16.9˚	32.3˚ ± 17.7˚	14.7˚
	2XB21	149.3˚ ± 10.2˚	130.0˚ ± 8.7˚	19.3˚ ± 13.5˚	7.3˚
	B21T	155.6˚ ± 3.2˚	129.2˚ ± 14.3˚	26.3˚ ± 14.7˚	11.4˚
	2XB21T	155.5˚ ± 4.3˚	136.9˚ ± 12.4˚	18.6˚ ± 13.1˚	6.6˚
Glass	***B21***	152.3˚ ± 5.0˚	122.6˚ ± 18.9˚	29.6˚ ± 19.6˚	18.0˚
	2XB21	155.9˚ ± 3.2˚	127.8˚ ± 15.2˚	28.1˚ ± 15.5˚	20.4˚
	B21T	146.0˚ ± 11.6˚	106.1˚ ± 17.4˚	39.9˚ ± 20.9˚	8.5˚
	2XB21T	147.4˚ ± 4.7˚	120.9˚ ± 16.1˚	26.4˚ ± 16.8˚	11.2˚

SUMMARY

We have shown that a newly developed SH coating formulation can withstand prolonged periods of wear and exposure to water. The results discussed show considerably improved durability when compared to previously studied coatings which were sensitive to light amounts of abrasion or exposure to water for ~5 minutes. Even after 240 minutes of abrasive wear and 5.5 hours of immersion in water, the tested samples remain hydrophobic with excellent repellency and good mobility as described.

ACKNOWLEDGMENTS

We thank Andrew Milne and Maryam Mohseni for their useful discussions, assistance with the collection of data and for the polymeric composite samples provided. Authors also thank DND, NSERC and Canada Research Chair Program for their financial support.

REFERENCES

1. Chang, H. C.; Yeo, L. Y. *Elektrokinetically Driven Microfluidics and Nanofluidics;* Cambridge University Press: New York, 2010.
2. Kirby, B. J. *Micro- and Nanoscale Fluid Mechanics: Transport in Microfluidic Devices;* Cambridge University Press: New York, 2010.
3. Barona, D.; Amirfazli, A. Producing a superhydrophobic paper and altering its repellency through ink-jet printing. *Lab Chip* **2011**. DOI: 10.1039/c0lc00335b
4. Balu, B.; Berry, A. D.; Hess, D. W.; Breedveld, V. Patterning of superhydrophobic paper to control the mobility of micro-liter drops for two-dimensional lab-on paper applications. *Lab Chip* **2009,** *9,* 3066-3075.
5. Antonini, C.; Carmona, F. J.; Pierce, E.; Marengo, M.; Amirfazli, A. General Methodology for Evaluating the Ashesion Force of Drops and Bubbles on Solid Surfaces. *Langmuir* **2009,** *25,* 6143-6154.
6. Pierce, E.; Carmona, F. J.; Amirfazli, A. Understanding of Sliding and Contact Angle Results in Tilted Plate Experiments. *Colloids Surfaces A* **2008,** *323,* 73-82.
7. Ishino, C.; Okumura, K.; Quere, D. Wetting Transitions on Rough Surfaces. *Europhys. Lett.* **2004,** *68* (3), 419-425.
8. Marmur, A. The Lotus Effect: Superhydrophobicity and Metastability. *Langmuir* **2004,** *20,* 3517-3519.
9. Shibuichi, A.; Onda, T.; Satoh, N.; Tsujii, K. J. Super Water-Repellent Surfaces Resulting from Fractal Structure. *Phys. Chem.* **1996,** *100*, 19512-19517.
10. Lafuma, A.; Quere, D. Superhydrophobic States. *Nat. Mater.* **2003,** *2,* 457-460.
11. Bayer, I. S.; Brown, A.; Steele, A.; Loth, E. Transforming Anaerobic Adhesives into Highly Durable and Abrasion Resistant Superhydrophobic Organoclay Nanocomposite Films: A New Hybrid Spray Adhesive for Tough Superhydrophobicity. *Applied Physics Express* **2009,** *2,* 125003.
12. Mohseni, M.; Mertiny, P.; Amirfazli, A. Electro-thermal icing mitigation system for polymeric composite airfoil. *International Mechanical Engineering Congress & Exposition*, Vancouver, 2010.
13. Li, W.; Amirfazli, A. Microtextured superhydrophobic surfaces: A thermodynamic analysis. *Advances Colloid Interface Sci.* **2007,** *132,* 51-68.
14. Stadler, A. F.; Kulik, G.; Sage, D.; Barbieri, L.; Hoffman, P. A Snake-Based Approach to Accurate Determination of Both Contact Points and Contact Angles. *Colloids Surfaces A* **2006,** *286,* 92-103.